

## Contribution of Soluble Minerals in Biochar to Pb<sup>2+</sup> Adsorption in Aqueous Solutions

De Chen,<sup>a,b,1</sup> Ruiyue Li,<sup>a,b,1</sup> Rongjun Bian,<sup>a,b</sup> Lianqing Li,<sup>a,b,\*</sup> Stephen Joseph,<sup>a,c</sup> David Crowley,<sup>d</sup> and Genxing Pan<sup>a,b</sup>

Biochar is widely used as an adsorbent to remove heavy metals from aqueous solutions. To investigate the contribution of soluble minerals (mainly anions) to Pb<sup>2+</sup> removal in solution, wheat straw biochar was washed with deionized water to remove soluble minerals. Batch adsorption was conducted using washed biochar (WBC) and unwashed biochar (BC) to adsorb Pb<sup>2+</sup>. After washing, the pH and ash content of biochar were reduced, while the specific surface area and total pore volume were increased. Adsorption kinetics of Pb<sup>2+</sup> onto BC and WBC were well fitted to the pseudo-second-order model ( $R^2 > 0.99$ ). Pb sorption on BC and WBC were better fit with the Langmuir model ( $R^2 = 0.96$  to  $0.97$ ) than the Freundlich model ( $R^2 = 0.71$  to  $0.87$ ). The Langmuir maximum adsorption capacity of Pb on BC was  $99.7 \text{ mg g}^{-1}$ , which was 4.5-fold higher than that on WBC when the initial solution pH was 5.0. The concentration of  $\text{SO}_4^{2-}$ ,  $\text{CO}_3^{2-}$ ,  $\text{SiO}_3^{2-}$ , and  $\text{PO}_4^{3-}$  in the equilibrium solution was reduced by 69, 89, 97, and 41%, respectively, with the increase of initial Pb<sup>2+</sup> concentration. The difference of Pb<sup>2+</sup> adsorption capacity between BC and WBC proved that the soluble anions in biochar play an important role in Pb<sup>2+</sup> sorption onto biochar.

*Keywords:* Adsorption; Biochar; Heavy metal; Soluble Mineral; Washings

*Contact information:* a: Institute of Resources, Ecosystem and Environment of Agriculture, and Center of Biochar and Green Agriculture, Nanjing Agricultural University, 1 Weigang, Nanjing, 210095, China; b: Jiangsu Collaborative Innovation Center for Solid Organic Waste Resource Utilization, Nanjing Agricultural University, 1 Weigang, Nanjing 210095, China; c: School of Materials Science and Engineering, University of New South Wales, Sydney, NSW 2052, Australia; d: Department of Environmental Sciences, University of California, Riverside, CA 92521, USA; \*Corresponding author: lqli@njau.edu.cn

1. These authors contributed to the work equally and should be regarded as co-first authors

### INTRODUCTION

Lead (Pb) contamination in waters and soils is an important environmental concern because of its toxicity to humans and other living organisms (Förstner and Wittmann 1979; Duruibe *et al.* 2007). Waters often contain potentially harmful levels of Pb due to unreasonable discharge of wastewater from industrial activities such as mining, electroplating, and battery manufacturing (Förstner and Wittmann 1979). It is urgent and necessary to treat these Pb-contaminated effluents and waters. Adsorption is a simple, cost-effective, and eco-friendly technique to remove Pb from wastewater (Bailey *et al.* 1999; Babel and Kurniawan 2003; Mohammed *et al.* 2011; Inyang *et al.* 2012). Biochar is an effective and low-cost adsorbent to remove both organic and inorganic pollutants from aqueous solutions (Inyang *et al.* 2015; Tan *et al.* 2015; Zhu *et al.* 2016).

Biochar is derived from pyrolyzing biomass under oxygen-limited conditions, and it consists of organic and mineral phases with abundant functional groups and minerals (Lehmann and Joseph 2009). Under the current environmental perspectives, biochar is

considered as a multi-functional bioresource for carbon sequestration (Lehmann 2007), greenhouse gas mitigation (Zhang *et al.* 2010), soil fertility promotion (Zheng *et al.* 2013), and for controlling environmental pollutants in soils and waters (Mohan *et al.* 2014; Nartey and Zhao 2014; Chen *et al.* 2015). Biochar effectively absorbs and removes  $Pb^{2+}$  from aqueous solutions (Zhang *et al.* 2013b; Cui *et al.* 2015; Elaigwu *et al.* 2014; Yang *et al.* 2014), while different components of biochar have differing contributions. The possible mechanisms of heavy metal sorption on biochar are summarized in recent review articles (Mohan *et al.* 2014; Inyang *et al.* 2015; Tan *et al.* 2015). Surface functional groups and minerals on biochar are two key factors determining heavy metal adsorption. The functional groups on the surface of biochar interact with heavy metals through electrostatic attraction, ion exchange, and surface complexation (Uchimiya *et al.* 2011; Tan *et al.* 2015). Lu *et al.* (2012) found that 32.8 to 42.3% of the total sorbed Pb was attributable to coordination with carboxyl and hydroxyl functional groups on biochar. On the other hand, precipitates (*e.g.*,  $Pb(OH)_2$ ,  $PbCO_3$ ,  $\beta$ - $Pb_9(PO_4)_6$ , and  $5PbO \cdot P_2O_5 \cdot SiO_2$ ) that form between  $Pb^{2+}$  and the minerals on biochar play an important role in Pb removal (Ryan *et al.* 2001; Cao *et al.* 2009; Lu *et al.* 2012). Cao *et al.* (2009) reported that precipitation accounted for 84 to 87% of Pb sorption on a dairy-manure derived biochar. Lu *et al.* (2012) also reported that co-precipitation or complex of  $Pb^{2+}$  on the biochar mineral surface accounted for 58 to 62% of the total absorbed Pb. These results indicate that minerals in biochar may have an important contribution on heavy metal removal from aqueous solutions (Tan *et al.* 2015; Wang *et al.* 2015).

However, some studies imply that the amount of Pb precipitation formed on biochar was not totally in proportion to its mineral content, as the precipitates formed as a result of the dissolution of anions such as  $CO_3^{2-}$ ,  $PO_4^{3-}$ , and  $Cl^-$  from biochar (Lu *et al.* 2012; Ding *et al.* 2014b; Wang *et al.* 2015). Wang *et al.* (2015) found a poor correlation between sorbed  $Pb^{2+}$  and ash content of biochars, indicating the sorption attributed to precipitation was not dependent on total mineral content. Thus, the formation of precipitates may depend on the content of soluble minerals (mainly anions) in biochar.

Removing soluble minerals from biochar is a good way to determine the contribution of these minerals to heavy metal removal. There are few studies reporting the changes of pollutant removal efficiency after biochar de-mineralization. Zhang *et al.* (2013a) reported that the adsorption of pesticide (carbaryl and atrazine) increased greatly on the deashed biochar compared with the original biochar. Wang *et al.* (2015) found a dramatic decrease of  $Pb^{2+}$  sorption on demineralized biochar treated by 1 M HCl compared with untreated biochar. Chen *et al.* (2012) used HCl and HF to remove the minerals on rice straw biochar and found that the Pb adsorption capacity of the deashed biochar was dramatically decreased compared with the original biochar. However, it was reported that acid could react with biochar components during washing, which may change the properties of biochar (Chen *et al.* 2012; Guo *et al.* 2014), while water was recommended to remove the soluble components with the least influence on biochar.

As there are few studies reporting on the contribution of the water-soluble minerals in biochar on  $Pb^{2+}$  adsorption, it was hypothesized in the present study that the soluble minerals (mainly anions) in biochar played an important role in Pb adsorption. Deionized water was used to remove the soluble minerals to determine the differences of Pb absorption capacity and confirm the contribution of soluble minerals on  $Pb^{2+}$  removal in solutions. The anions ( $CO_3^{2-}$ ,  $PO_4^{3-}$ ,  $SO_4^{2-}$ , and  $SiO_4^{3-}$ ) in the equilibrium solution were determined to evaluate their potential contribution to Pb precipitation.

## EXPERIMENTAL

### Preparation of Biochar

Wheat straw was obtained from Nanjing Qinfeng Straw Technology Co. Ltd. In Nanjing, Jiangsu Province, China. Wheat straw was washed with deionized water to remove the attached dust and oven-dried at 75 °C. The dried feedstock was then ground, passed through a 2 mm sieve, and placed in stainless steel kilns (the diameter and height were 10 cm and 15 cm, respectively).

The kilns were placed into a muffle furnace and pyrolyzed with a heating rate of 5 °C min<sup>-1</sup>. The maximum pyrolysis temperature of 450 °C was held for 30 min. The kilns were moved to a vacuum dryer to isolate air until they reached room temperature. The yield of biochar was 34.7% of the original biomass. The derived biochar was passed through a 0.149 mm sieve, homogenized, and divided into two parts. One part was sealed in an airtight plastic bag and denoted as BC for analysis; the other part was washed with deionized water and then denoted as WBC (washed biochar).

### Washing Procedure of Biochar

A total of 1.0 g biochar was added to a 500 mL flask with 300 mL deionized water. The mixture was shaken for 30 min at 180 rpm and vacuum filtered through a 30-µm membrane. The ions and anions in the filtrate were determined. The procedure was repeated 7 to 8 times until the ions and anions in the filtrate were below the detection limit. The washed biochar was oven-dried at 55 °C for 24 h.

### Characterization of Biochar

The analysis of biochar properties including pH, organic carbon (OC), ash, and anions (SO<sub>4</sub><sup>2-</sup>, PO<sub>4</sub><sup>3-</sup>, CO<sub>3</sub><sup>2-</sup>, and HCO<sub>3</sub><sup>-</sup>) were conducted following the procedures described by Lu (2000). The pH was determined using a Mettler Toledo Seveneasy precision pH meter (Mettler-Toledo AG, Analytical; Schwerzenbach, Switzerland) with a water-biochar ratio of 20:1 (v:m). Organic carbon content (OC) was analyzed by wet digestion of potassium dichromate.

The ash content in biochars was determined by heating biochar in a muffle furnace at 750 °C for 6 h (Wang *et al.* 2015). SO<sub>4</sub><sup>2-</sup> was determined by barium chromate spectrophotometry; PO<sub>4</sub><sup>3-</sup> was determined by the isobutyl alcohol extraction- molybdenum blue colorimetric method. SiO<sub>3</sub><sup>2-</sup> was determined by the molybdenum blue colorimetric method; CO<sub>3</sub><sup>2-</sup> was determined by neutralization titration.

Surface area and pore structure were investigated using a V-Sorb 2800 nitrogen adsorption system (Beijing Jinaipu General Instrument Co., Ltd, Beijing, China). Fourier transform infrared spectroscopy (FTIR) was used to characterize the surface functional groups on the biochars. The spectra of samples were determined from 400 to 4000 cm<sup>-1</sup> wave number by KBr method on a Bruker TENSOR27 FTIR spectrometer (Bruker Optics Inc., Billerica, MA, USA).

Scanning electron microscopy (SEM) and transmission electron microscopy (TEM) with energy dispersive X-ray spectroscopy (EDS) were used to examine the surface structure and elemental composition and were described by previous studies (Joseph *et al.* 2013; Bian *et al.* 2014). The basic properties of BC and WBC are listed in Table 1.

**Table 1.** Properties of Biochar before and After Washing

Biochar	pH	Ash (%)	OC (g kg <sup>-1</sup> )	Specific Surface Area (m <sup>2</sup> g <sup>-1</sup> )	Total Pore Volume (m <sup>3</sup> g <sup>-1</sup> )	Average Pore Size (nm)
BC	9.93	28.6	630	30.0	0.052	7.00
WBC	7.02	14.2	617	47.9	0.079	6.63

### Adsorption Experiment

A stock solution of 10 g L<sup>-1</sup> Pb<sup>2+</sup> was prepared using analytical reagent Pb(NO<sub>3</sub>)<sub>2</sub> and was diluted to 10 to 1000 mg L<sup>-1</sup>. All tested Pb<sup>2+</sup> solutions contained 0.01 M NaNO<sub>3</sub> as a background electrolyte, and the pH was pre-adjusted to 5.0 with 0.1 M HNO<sub>3</sub> and NaOH solutions. For the kinetic adsorption test, 0.1000 g biochar was added to a 50 mL conical flask with 25 mL of Pb<sup>2+</sup> solution (400 mg L<sup>-1</sup>). All the experimental treatments were conducted in duplicate and the average values were presented. The mixture was agitated on a thermostatic reciprocating shaker at 180 rpm and 25 °C for 5 min, 15 min, 30 min, 1 h, 2 h, 4 h, 8 h, or 12 h. The solid and liquid phases were separated immediately by filtration, and the Pb concentration in the filtrate was determined. For isothermal adsorption, 0.1000 g biochar was added to a 50 mL conical flask with 25 mL of Pb<sup>2+</sup> solutions ranging in concentration from 10 to 1000 mg L<sup>-1</sup>. The mixture was shaken at 180 rpm and 25 °C for 12 h. After shaking, solid and liquid phases were separated by filtration. The Pb concentration in the filtrate was determined by atomic absorption spectrophotometer (AAS, A3, Persee Analytical Instruments, Beijing, China). The effect of initial solution pH on Pb adsorption was determined by added 0.1000 g biochar to a 50 mL conical with 25 mL of 400 mg L<sup>-1</sup> Pb<sup>2+</sup> solution. The pH of the solutions was pre-adjusted to 2.5 to 6.5 with 0.1 M HNO<sub>3</sub> and NaOH. The mixture was shaken and filtered, and the concentration of Pb in equilibrium solutions were determined as described above. Blanks without biochar or Pb<sup>2+</sup> were used during the adsorption process. All of the reagents in this research were purchased from Nanjing Shoude laboratory equipment Co., Ltd, Nanjing, China. The SO<sub>4</sub><sup>2-</sup> in the filtrate was determined by barium chromate spectrophotometry; PO<sub>4</sub><sup>3-</sup> was determined by the isobutyl alcohol extraction- molybdenum blue colorimetric method. SiO<sub>3</sub><sup>2-</sup> was determined by the molybdenum blue colorimetric method; CO<sub>3</sub><sup>2-</sup> and HCO<sub>3</sub><sup>-</sup> were determined by neutralization titration.

### Statistical Analysis of the Experimental Data

Pseudo-first-order (Eq. 1), pseudo-second-order (Eq. 2), and intraparticle diffusion (Eq. 3) kinetic models were used to simulate the kinetics of Pb sorption to biochar (Weber and Morris 1962; Inyang *et al.* 2012),

$$Q_t = Q_e (1 - e^{-k_1 t}) \quad (1)$$

$$Q_t = \frac{k_2 Q_e^2 t}{1 + k_2 Q_e^2 t} \quad (2)$$

$$Q_t = k_p t^{0.5} + C \quad (3)$$

where  $Q_t$  (mg g<sup>-1</sup>) and  $Q_e$  (mg g<sup>-1</sup>) are the amounts of Pb sorbed at time  $t$  and at equilibrium, respectively. The parameters  $k_1$  (h<sup>-1</sup>),  $k_2$  (mg g<sup>-1</sup> h<sup>-1</sup>), and  $k_p$  (mg g<sup>-1</sup> h<sup>-0.5</sup>) are the first-order, second-order, and intraparticle diffusion apparent sorption rate constants, respectively.

The Langmuir (Eq. 4) and Freundlich (Eq. 5) models were used to evaluate Pb sorption on biochar,

$$\frac{Q_e}{Q_{\max}} = \frac{bC_e}{1 + bC_e} \quad (4)$$

$$Q_e = KC_e^{\frac{1}{n}} \quad (5)$$

where  $Q_e$  is the amount of Pb adsorbed to biochar at equilibrium ( $\text{mg g}^{-1}$ ),  $Q_{\max}$  is the maximum adsorption capacity of biochar on Pb ( $\text{mg g}^{-1}$ ),  $C_e$  is Pb concentration in solution at equilibrium ( $\text{mg L}^{-1}$ ),  $b$  is Langmuir constant related to sorption intensity ( $\text{L mg}^{-1}$ ), and  $K$  and  $n$  are empirical Freundlich constant related to sorption capacity ( $\text{mg}^{(1-n)} \text{L}^n/\text{g}$ ) and sorption intensity, respectively.

## RESULTS AND DISCUSSION

### Characteristics of Biochar Before and After Washing

The basic properties of wheat straw derived biochar (BC) and water washed biochar (WBC) are listed in Table 1. The nature of biochar was alkaline ( $\text{pH} = 9.93$ ), and it became neutral (7.02) after washing with deionized water. Biochars derived from agronomic wastes are usually alkaline due to the formation of alkali such as carbonates during pyrolysis (Yuan *et al.* 2011). Ash content in WBC was 50% lower than BC, indicating that nearly half of minerals in wheat straw biochar was water soluble and leachable. The organic carbon (OC) content was slightly lower (about 2%) in WBC than in BC. Wu *et al.* (2011) also reported that water leaching can remove small amounts (< 2%) of organic carbon of mallee-derived biochar. The specific surface area and total pore volume were increased by 60% and 52%, respectively after washing, while there was little change of the average pore size (Table 1). The increased SSA and TPV of WBC may be attributed to the removal of soluble components such as ash and organic carbon in pores and surface of biochar during washing.

### Adsorption of Pb on BC and WBC

#### Adsorption kinetics

Pseudo-first-order (PF), pseudo-second-order (PS), and intraparticle diffusion (IPD) models are three kinetic models frequently used to study the adsorption of contaminants by biochar. Table 2 illustrates the parameters of  $\text{Pb}^{2+}$  sorbed onto BC and WBC through three kinetic models.

**Table 2.** Regression Parameters of Kinetics Equation for the Adsorption of  $\text{Pb}^{2+}$  onto BC and WBC

Biochar	Pseudo-first-order model			Pseudo-second-order model			Intraparticle diffusion model	
	$Q_e$ ( $\text{mg}\cdot\text{g}^{-1}$ )	$k_1$ ( $\text{h}^{-1}$ )	$R^2$	$Q_e$ ( $\text{mg}\cdot\text{g}^{-1}$ )	$k_2$ ( $\text{mg}\cdot(\text{g}\cdot\text{h})^{-1}$ )	$R^2$	$k_p$ ( $\text{mg}\cdot\text{g}^{-1}\cdot\text{h}^{-0.5}$ )	$R^2$
BC	35.15	0.1817	0.8625	95.24	0.0441	0.9994	13.58	0.8632
WBC	11.50	0.2660	0.9151	25.58	0.1012	0.9972	4.213	0.9270

Note:  $Q_e$  ( $\text{mg g}^{-1}$ ) is the amount of  $\text{Pb}^{2+}$  sorbed at equilibrium;  $k_1$  ( $\text{h}^{-1}$ ),  $k_2$  ( $\text{mg}\cdot(\text{g}\cdot\text{h})^{-1}$ ), and  $k_p$  ( $\text{mg g}^{-1} \text{h}^{-0.5}$ ) are the first-order, second-order, and intraparticle diffusion apparent sorption rate constants, respectively.

There was a rapid initial adsorption during the first 2 h for BC (accounting for 85% of total sorption capacity), which slowly reached equilibrium in 12 h. Thus, the sorption process of  $\text{Pb}^{2+}$  to wheat straw biochar (BC) was divided into fast and slow stages, which was similar to many other studies (Ding *et al.* 2014a; Wang *et al.* 2015). However, it was not easy to distinguish the fast and slow stages of  $\text{Pb}^{2+}$  sorption on WBC, which gradually reached equilibrium in 12 h (Fig. S1).

$\text{Pb}^{2+}$  adsorption by BC and WBC was well fitted to the three kinetic models ( $R^2 > 0.86$ ) generally, while PS was the best model to simulate Pb sorption on BC and WBC with their  $R^2 > 0.99$  (Table 2). The second-order apparent sorption rate constant ( $k_2$ ) of WBC was 2.3-fold higher than that of BC (Table 2), demonstrating a faster Pb adsorption process on washed biochar than on original biochar. The electrostatic ion exchange between  $\text{Pb}^{2+}$  and acidic oxygen functional groups is fast, reaching equilibrium in a few minutes (Lu *et al.* 2012).  $\text{Pb}^{2+}$  can precipitate with anions (*e.g.*,  $\text{PO}_4^{3-}$  and  $\text{CO}_3^{2-}$ ) released from minerals in biochars during adsorption in solution, so the dissolution rate of these anions may be the rate-limiting step (Lu *et al.* 2012; Wang *et al.* 2015). In the present study, the water-soluble minerals were removed in WBC (Table 1), while the oxygen functional groups were not significantly changed (Fig. S2). This was why the adsorption rate was faster on WBC than BC. Intraparticle diffusion can also be a rate-limiting step for metal adsorption on biochars, which occurs in two steps (Wang *et al.* 2011, 2015). The first step is mass transfer of metal ions (such as  $\text{Pb}^{2+}$ ) from bulk solution to the biochar surface, which is faster, and the second step is intraparticle diffusion of ions, which is slower (Ding *et al.* 2014a; Wang *et al.* 2015). The equilibrium adsorption capacity of WBC was 73% lower than BC, which was attributed to the loss of soluble minerals in biochar.

### Isothermal adsorption

Figure 1 and Table 3 illustrate that the isothermal adsorption of  $\text{Pb}^{2+}$  on BC and WBC were better fitted with the Langmuir model ( $R^2 = 0.96$  to  $0.97$ ) than the Freundlich model ( $R^2 = 0.71$  to  $0.87$ ), implying a monolayer adsorption of Pb on biochar with a homogeneous surface (Foo and Hameed 2010; Hu *et al.* 2011). Equilibrium adsorption capacity increased sharply with the increase of initial  $\text{Pb}^{2+}$  concentration in solution, and it remained stable when the initial Pb concentration increased to a threshold level (Fig. 1).

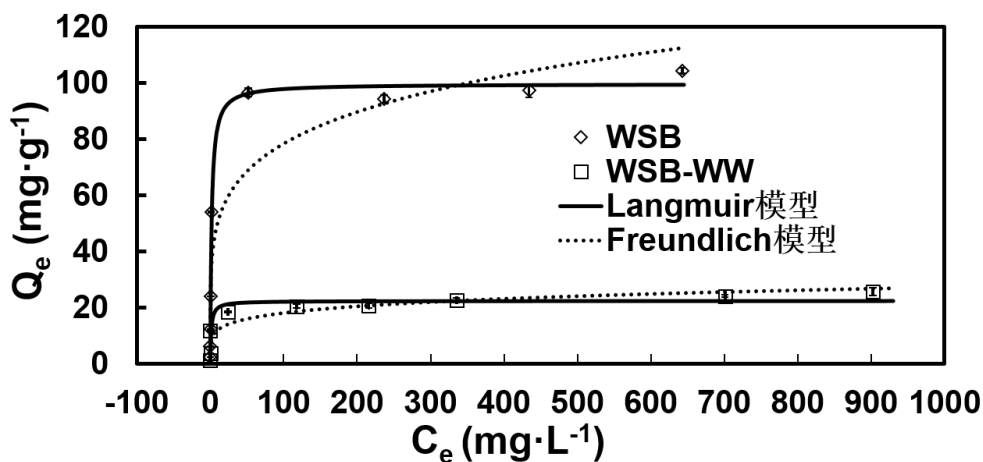


**Fig. 1.** Adsorption isotherm of  $\text{Pb}^{2+}$  onto original biochar (BC) and water washed biochar (WBC).  $Q_e$  is the amount of  $\text{Pb}^{2+}$  sorbed to biochar at equilibrium ( $\text{mg g}^{-1}$ ), and  $C_e$  is  $\text{Pb}^{2+}$  concentration in solution at equilibrium ( $\text{mg L}^{-1}$ ).

The Langmuir maximum adsorption capacity ( $Q_{max}$ ) of BC was 99.7 mg g<sup>-1</sup>, which was 4.5-fold higher than WBC (Table 3). This indicates that the adsorption capacity was greatly reduced when the water-soluble minerals were removed from the original biochar.

**Table 3.** Regression Parameters of Langmuir and Freundlich Models for Adsorption Isotherm of Pb<sup>2+</sup> onto BC and WBC

Biochar	Langmuir			Freundlich		
	$Q_{max}$ (mg·g <sup>-1</sup> )	$b$ (L·mg <sup>-1</sup> )	R <sup>2</sup>	$K$ (mg <sup>1-N</sup> ·g <sup>-1</sup> ·L <sup>-N</sup> )	$n$	R <sup>2</sup>
BC	99.7	0.54	0.97	32.1	5.16	0.87
WBC	22.4	0.77	0.96	7.96	5.62	0.71

Note:  $Q_{max}$  is the maximum adsorption capacity of biochar on Pb (mg g<sup>-1</sup>),  $b$  is the Langmuir constant related to sorption intensity (L mg<sup>-1</sup>),  $K$  (mg<sup>1-N</sup>·g<sup>-1</sup>·L<sup>-N</sup>), and  $n$  and  $N$  are the empirical Freundlich constant related to sorption capacity and sorption intensity, respectively.

#### Effect of initial solution pH on Pb sorption on BC and WBC

Figure 2 shows the effects of initial solution pH on Pb<sup>2+</sup> sorption on BC and WBC. When the initial solution pH was 2.5, the equilibrium adsorption capacity of BC and WBC was very low, especially for the washed biochar. With increasing initial solution pH,  $Q_e$  was sharply increased to a relative stable range for BC (73 to 80 mg kg<sup>-1</sup>) and WBC (13 to 20 mg kg<sup>-1</sup>). The equilibrium Pb adsorption capacity of BC was more than 5-fold higher than that of WBC at higher initial pH.

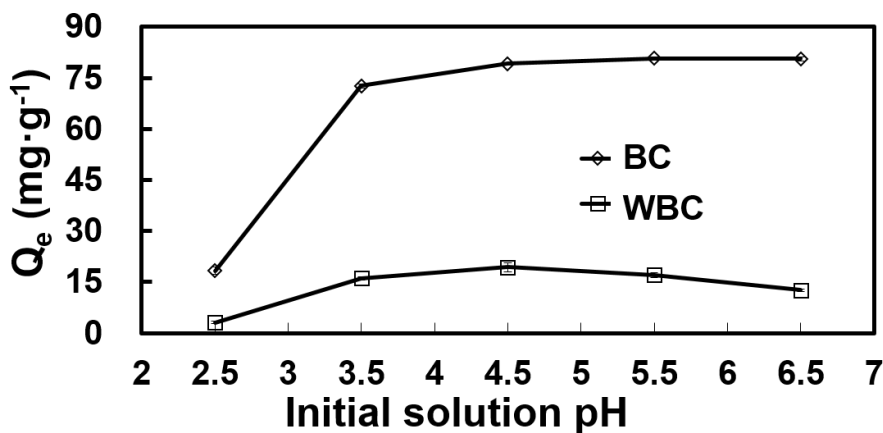


**Fig. 2.** Effects of initial solution pH on Pb<sup>2+</sup> adsorption capacity by original biochar (BC) and water washed biochar (WBC).  $Q_e$  is the amount of Pb<sup>2+</sup> sorbed to biochar at equilibrium (mg g<sup>-1</sup>).

#### Effect of Soluble Minerals on Pb Adsorption on Biochar

##### Changes of anions in equilibrium solution

Figure 3 shows the concentration of anions in equilibrium solutions of BC. The initial Pb<sup>2+</sup> concentrations ranged from 0 to 1000 mg L<sup>-1</sup>. When biochar was added to the solution with 0 mg L<sup>-1</sup> Pb, the concentration of SO<sub>4</sub><sup>2-</sup>, CO<sub>3</sub><sup>2-</sup>, SiO<sub>3</sub><sup>2-</sup>, and PO<sub>4</sub><sup>3-</sup> in the equilibrium solution were 107.51, 136.88, 91.12, and 4.44 mg L<sup>-1</sup>, respectively; however, the concentrations of the corresponding anions in WBC solution were 33.36, 15.25, 2.95, and 2.64 mg L<sup>-1</sup> (data not shown). Thus, deionized water removed most of the soluble anions after washing. Anion concentrations at equilibrium were dramatically decreased with the increase of initial Pb concentration in BC solutions (Fig. 3). The concentration of

$\text{SO}_4^{2-}$  and  $\text{PO}_4^{3-}$  decreased to nearly 0  $\text{mg L}^{-1}$  when the initial Pb concentration increased to 1000 and 200  $\text{mg L}^{-1}$ , respectively. The concentration of  $\text{CO}_3^{2-}$  was dramatically reduced from 127 to 6  $\text{mg L}^{-1}$ , while  $[\text{SiO}_3^{2-}]$  was decreased from 91  $\text{mg L}^{-1}$  to 20  $\text{mg L}^{-1}$ , respectively, when the initial Pb concentration increased from 0 to 1000  $\text{mg L}^{-1}$ . The anions in WBC equilibrium solution were undetectable, so the data are not listed. According to the decreasing amount of these anions, the predicted contribution of each anion to Pb removal through precipitation occurred in the following order:  $\text{CO}_3^{2-} > \text{SO}_4^{2-} > \text{SiO}_3^{2-} > \text{PO}_4^{3-}$ . However, the anion content changes in different biochars according to feedstock and pyrolysis conditions should be noted.

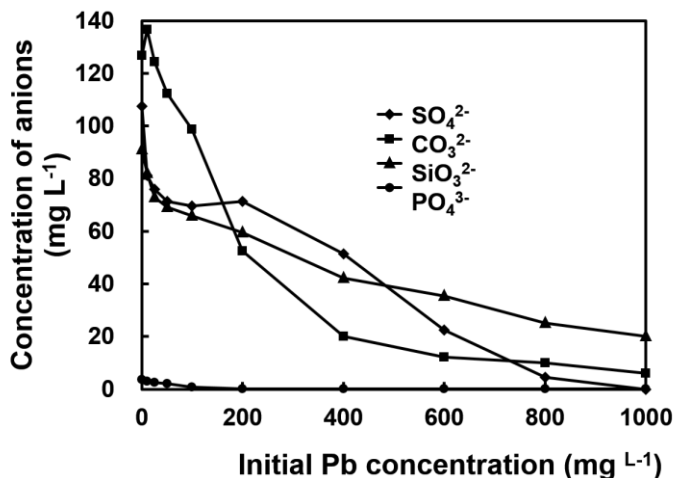


**Fig. 3.** Concentration of  $\text{SO}_4^{2-}$ ,  $\text{CO}_3^{2-}$ ,  $\text{SiO}_3^{2-}$  and  $\text{PO}_4^{3-}$  in the equilibrium solution of original biochar with various initial  $\text{Pb}^{2+}$  concentration

The decrease of anions in equilibrium solutions with increasing initial  $\text{Pb}^{2+}$  concentration may be attributed to the formation of precipitates of Pb with these anions. Xu *et al.* (2013) found that  $\text{PO}_4^{3-}$  and  $\text{CO}_3^{2-}$  were responsible for metal sorption to dairy manure-derived biochar through formation of precipitates. These could also be reflected by the changes of FTIR spectra (Fig. S2), SEM-EDS (Fig. S3), and TEM images (Fig. S4) after  $\text{Pb}^{2+}$  adsorption. In Fig. S2, the peaks related to Si-O-Si ( $1104$ ,  $802$ , and  $467$   $\text{cm}^{-1}$ ) became weak after Pb adsorption of both BC and WBC, indicating  $\text{SiO}_2$  on biochar was associated with Pb, probably due to precipitation. Fig. S3 shows the SEM-EDS images of BC and WBC; A and B are the SEM images of the BC surface at a larger and smaller area, respectively, after Pb adsorption. C and D are the corresponding EDS spectra collected from the boxed regions. There were also Pb peaks on the BC surface associated with elements such as Si, P, C, and O. For WBC, there were no Pb peaks detected, although Si, C, and O peaks appeared. Similarly, the TEM images and the corresponding EDS spectra also demonstrated that Pb was present with C, O, Si, and even P in BC (Fig. S4). Although there were Pb peaks in the TEM-EDS spectra of WBC, the abundance was much lower than in BC (Fig. S4). The information above demonstrates that  $\text{Pb}^{2+}$  was associated with anions through possible precipitation.

#### *Changes of anions in equilibrium solutions with various initial pH*

Figure 4 shows the concentration of anions in BC and WBC solution at different initial pH with and without  $\text{Pb}^{2+}$ . When pH was 2.5,  $\text{CO}_3^{2-}$  and  $\text{SiO}_3^{2-}$  released from BC

were only 23.79 and 22.51 mg L<sup>-1</sup>, respectively; there were similar concentrations of the two anions in Pb(NO<sub>3</sub>)<sub>2</sub> solution. This result indicates that there was no precipitation when the solution was very acidic. When pH was in the range of 3.5 to 6.5, CO<sub>3</sub><sup>2-</sup> and SiO<sub>3</sub><sup>2-</sup> released from BC were nearly 130 and 110 mg L<sup>-1</sup>, respectively, while they decreased to about 33 and 56 mg L<sup>-1</sup> when Pb(NO<sub>3</sub>)<sub>2</sub> was added. There was little effect of pH on SO<sub>4</sub><sup>2-</sup> release in BC solution; it was decreased by nearly 50% in when Pb(NO<sub>3</sub>)<sub>2</sub> was added regardless of pH. The concentration of CO<sub>3</sub><sup>2-</sup>, SiO<sub>3</sub><sup>2-</sup>, and SO<sub>4</sub><sup>2-</sup> in solutions with WBC was much lower than in BC solutions.

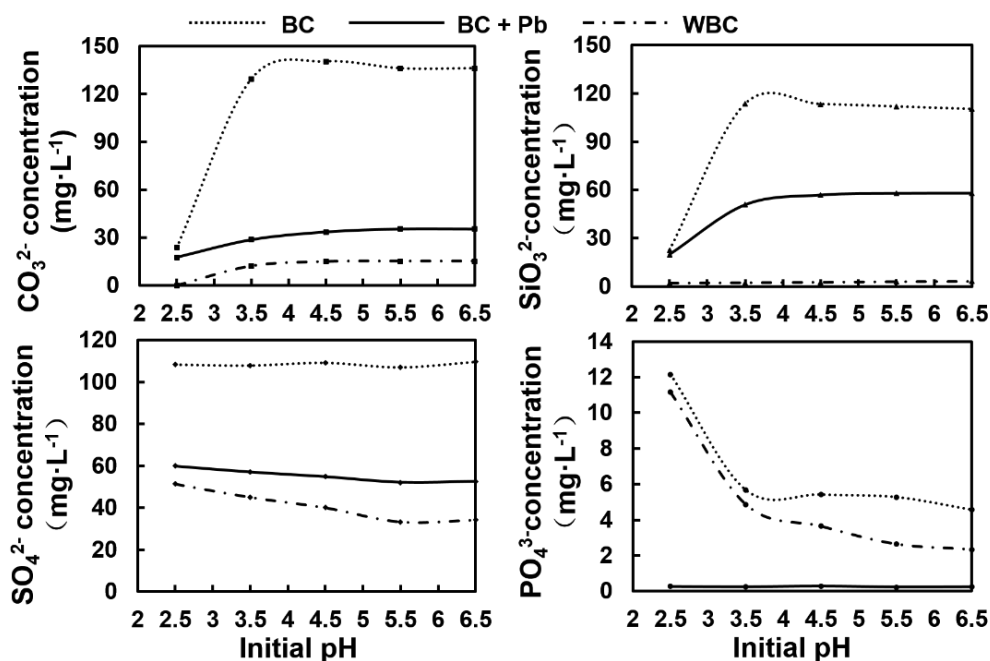


**Fig. 4.** Concentration of anions at equilibrium solution with different initial pH. BC means only original biochar solution with no Pb<sup>2+</sup> added; BC+Pb means original biochar solution with Pb<sup>2+</sup> added; WBC means water washed biochar solution without Pb<sup>2+</sup> added.

The concentration of PO<sub>4</sub><sup>3-</sup> was lower than other anions. The PO<sub>4</sub><sup>3-</sup> concentration also decreased with the increase of initial solution pH. The concentration of PO<sub>4</sub><sup>3-</sup> released from BC was 12.15 mg L<sup>-1</sup> at pH 2.5 and decreased to nearly 5 mg L<sup>-1</sup> at pH 3.5 to 6.5. There were similar PO<sub>4</sub><sup>3-</sup> concentrations in solution with WBC and BC at pH 2.5 and 3.5; there was much less in WBC solution than BC when the initial pH was 4.5 to 6.5. This was possibly because the phosphates from the original biochar, which were insoluble in water, became dissolved under acidic conditions (pH 2.5 and 3.5 in this study). However, when Pb(NO<sub>3</sub>)<sub>2</sub> was added, the PO<sub>4</sub><sup>3-</sup> concentration was reduced to nearly 0.2 mg L<sup>-1</sup> regardless of the change of solution pH.

### Adsorption Mechanisms

Pb precipitates have been identified by XRD on biochar after adsorption, including lead hydroxides (Pb(OH)<sub>2</sub>), lead carbonate (PbCO<sub>3</sub>), lead phosphate (β-Pb<sub>9</sub>(PO<sub>4</sub>)<sub>6</sub>), lead sulfate (Pb<sub>2</sub>(SO<sub>4</sub>)O), and other complex minerals such as Pb<sub>3</sub>(CO<sub>3</sub>)<sub>2</sub>(OH)<sub>2</sub>, 5PbO·P<sub>2</sub>O<sub>5</sub>·SiO<sub>2</sub>, 3PbCO<sub>3</sub>·2Pb(OH)<sub>2</sub>·H<sub>2</sub>O, Pb<sub>4</sub>(CO<sub>3</sub>)<sub>2</sub>(SO<sub>4</sub>)(OH)<sub>2</sub>, and Pb<sub>5</sub>(PO<sub>4</sub>)<sub>3</sub>OH (Cao *et al.* 2009; Lu *et al.* 2012; Wang *et al.* 2015). In the present study, the FTIR spectra, SEM-EDS, and TEM-EDS from Pb-loaded BC showed that Pb was associated with Si, C, P, and

S, which implied possible precipitation of  $\text{Pb}^{2+}$  with silica,  $\text{PO}_4^{3-}$ ,  $\text{CO}_3^{2-}$ , and  $\text{SO}_4^{2-}$ . The formation of precipitates is mainly due to the dissolution of anions from the minerals in biochar (Cao *et al.* 2009; Lu *et al.* 2012; Ding *et al.* 2014b). In a previous adsorption study using dairy manure derived biochar, Cao *et al.* (2009) found that dissolved P decreased with increasing Pb concentration as Pb phosphate formed. Wang *et al.* (2015) also reported that the concentration of  $\text{PO}_4^{3-}$  in solution decreased after  $\text{Pb}^{2+}$  adsorption by biochar. In the present study, the concentration of anions including  $\text{CO}_3^{2-}$ ,  $\text{SO}_4^{2-}$ , and  $\text{SiO}_3^{2-}$  in solution was dramatically reduced as well as  $[\text{PO}_4^{3-}]$  with the increase of initial  $\text{Pb}^{2+}$  concentration after adsorption (Fig. 3), implying the precipitation of these anions with  $\text{Pb}^{2+}$ . Previous studies showed a dramatic decrease of Pb adsorption capacity of biochars after demineralization with acid (Chen *et al.* 2012; Wang *et al.* 2015). In the present study, the  $\text{Pb}^{2+}$  adsorption capacity was reduced by 78% when biochar was washed with water compared with unwashed biochar. Xu and Chen (2014) found that the relative contribution of water-soluble matter to the decrease of Cd in solution was more than 71% for two rice-bran derived biochars. After washing with deionized water, soluble minerals were removed (Table 1), while there was little impact on organic functional groups of biochar (Fig. S2). Therefore, the decrease of  $\text{Pb}^{2+}$  adsorption capacity of WBC compared to BC was mainly attributed to the loss of soluble minerals (mainly anions). This confirmed the contribution of soluble anions on biochar to  $\text{Pb}^{2+}$  removal, which was also evidenced by the decrease of anions in the solution after adsorption (Fig. 3). However, the situation may vary among different type of biochars, as they have various mineral content. In addition, some ions in biochar could react with the anions besides Pb. Qian *et al.* (2016) in found that the released anions (such as  $\text{OH}^-$ ,  $\text{CO}_3^{2-}$ ,  $\text{PO}_4^{3-}$ , and Si species) from biochar can react with  $\text{Ca}^{2+}$ ,  $\text{Mg}^{2+}$  as well as  $\text{Zn}^{2+}$  in solution.

On the other hand, the solution pH can also affect the adsorption performance of biochar. However, the effects of pH on heavy metal adsorption capacity by biochar were different in different pH ranges. In this study, the lower pH of WBC after washing may contribute to reduce Pb adsorption capacity. Furthermore, the losses of very fine-particle - size materials and some water-soluble organic by washing also may lead to overestimation of the contribution of water-soluble minerals to Pb removal.

The oxygen functional groups on biochar are also responsible for heavy metal adsorption. The FTIR spectra peaks at 3410 and 1600  $\text{cm}^{-1}$  of WBC became weaker after Pb adsorption (Fig. S2), likely from complexes between  $-\text{COOH}$  or  $-\text{OH}$  and  $\text{Pb}^{2+}$ . However, there were no changes of these groups in BC after  $\text{Pb}^{2+}$  adsorption (Fig. S2). This result indicates that the role of oxygen functional groups in original biochar was minor compared with the mineral components. However, when the soluble minerals were removed,  $\text{Pb}^{2+}$  formed complexes with the functional groups. In this study, the pyrolysis temperature of biochar was 450 °C; the biochar possessed both aliphatic and aromatic groups (Fig. S2). The aromatic properties increase and aliphatic properties decrease with increasing pyrolysis temperature (Cantrell *et al.* 2012; Kloss *et al.* 2012). Pb- $\pi$  interaction could occur in biochar with aromatic structures (Wang *et al.* 2015). Furthermore, the peaks at 1104, 802, and 467  $\text{cm}^{-1}$  weakened in WBC after Pb loaded (Fig. S2), indicating that the insoluble silica that was not removed by water in biochar partly contributed to Pb removal.

Surface area and the porous structure of biochar influence the adsorption of heavy metals. In this study, the adsorption capacity of  $\text{Pb}^{2+}$  was reduced sharply, although the SSA and pore volume were increased after washing. Cao *et al.* (2009) indicated that Pb sorption in dairy-manure derived biochar was 6-fold higher in than a commercial activated carbon (AC), although the SSA of AC was 61 to 161 times that of BC. Kim *et al.* (2013)

reported that giant *Miscanthus* biochar derived at 600 °C had higher SSA (2-fold) and lower Cd adsorption capacity than biochar derived at 500 °C. These results demonstrated that the contribution of SSA and porous structure was minor in heavy metal adsorption, which was also supported by Tan *et al.* (2015).

## CONCLUSIONS

1. Wheat straw biochar effectively absorbed  $\text{Pb}^{2+}$  from aqueous solution. The adsorption kinetics of  $\text{Pb}^{2+}$  onto biochars were well fitted by a pseudo-second-order model ( $R^2 > 0.99$ ). Pb sorption on wheat straw biochar was best fitted with the Langmuir model ( $R^2 = 0.96$  to  $0.97$ ), with the maximum adsorption capacity ( $Q_{\max}$ ) of  $99.7 \text{ mg g}^{-1}$  of BC.
2. Deionized water removed the soluble minerals without changing the oxygen functional groups. The  $Q_{\max}$  of biochar was reduced by 73% after removal of soluble minerals from biochar when the initial solution pH was 5.0.
3. The concentration of  $\text{SO}_4^{2-}$ ,  $\text{CO}_3^{2-}$ ,  $\text{SiO}_3^{2-}$ , and  $\text{PO}_4^{3-}$  in the equilibrium solution was reduced by 69, 89, 97, and 41%, respectively, when the initial  $\text{Pb}^{2+}$  concentration was  $1000 \text{ mg L}^{-1}$ . This result proved the contribution of soluble minerals in biochar through formation of precipitates.

## ACKNOWLEDGMENTS

This study was financially supported by the National Non-profit Program by Ministry of Agriculture of China (201303095-11) and National Natural Science Foundation of China (41501353).

## REFERENCES CITED

- Babel, S., and Kurniawan, T. A. (2003). "Low-cost adsorbents for heavy metals uptake from contaminated water: A review," *Journal of Hazardous Materials* 97(1-3), 219-243. DOI: 10.1016/S0304-3894(02)00263-7
- Bailey, S. E., Olin, T. J., Bricka, R. M., and Adrian, D. D. (1999). "A review of potentially low-cost sorbents for heavy metals," *Water Research* 33(11), 2469-2479. DOI: 10.1016/S0043-1354(98)00475-8
- Bian, R. J., Joseph, S., Cui, L. Q., Pan, G. X., Li, L. Q., Liu, X. Y., Zhang, A., Rutledge, H., Wong, S. W., Chia, C., *et al.* (2014). "A three-year experiment confirms continuous immobilization of cadmium and lead in contaminated paddy field with biochar amendment," *Journal of Hazardous Materials* 272, 121-128. DOI: 10.1016/j.jhazmat.2014.03.017
- Cantrell, K. B., Hunt, P. G., Uchimiya, M., Novak, J. M., and Ro, K. S. (2012). "Impact of pyrolysis temperature and manure source on physicochemical characteristics of biochar," *Bioresource Technology* 107, 419-428. DOI: 10.1016/j.biortech.2011.11.084
- Cao, X. D., Ma, L. N., Gao, B., and Harris, W. (2009). "Dairy-manure derived biochar effectively sorbs lead and atrazine," *Environmental Science & Technology* 43(9),

- 3285-3291. DOI: 10.1021/es803092k
- Chen, D., Guo, H., Li, R. Y., Li, L. Q., Pan, G. X., Chang, A., and Joseph, S. (2016). "Low uptake affinity cultivars with biochar to tackle Cd-tainted rice - A field study over four rice seasons in Hunan, China," *Science of the Total Environment* 541, 1489-1498. DOI: 10.1016/j.scitotenv.2015.10.052
- Chen, Z. M., Fang, Y., Xu, Y. L., and Chen, B. L. (2012). "Adsorption of Pb<sup>2+</sup> by rice straw derived-biochar and its influential factors," *Acta Scientiae Circumstantiae* 32(4), 769-776 (in Chinese).
- Cui, L. Q., Yan, J. L., Li, L. Q., Quan, G. X., Ding, C., Chen, T. M., Yin, C. T., Gao, J. F., and Hussain, Q. (2015). "Does biochar alter the speciation of Cd and Pb in aqueous solution?" *BioResources* 10(1), 88-104. DOI: 10.15376/biores.10.1.88-104
- Ding, W. C., Dong, X. L., Ime, I. M., Gao, B., and Ma, L. Q. (2014a). "Pyrolytic temperatures impact lead sorption mechanisms by bagasse biochars," *Chemosphere* 105, 68-74. DOI: 10.1016/j.chemosphere.2013.12.042
- Ding, W. C., Peng, W. L., Zeng, X. L., and Tian, X. M. (2014b). "Effects of phosphorus concentration on Cr(VI) sorption onto phosphorus-rich sludge biochar," *Frontiers of Environmental Science & Engineering* 8(3), 379-385. DOI: 10.1007/s11783-013-0606-0
- Duruibe, J. O., Ogwuegbu, M. O. C., and Egwurugwu, J. N. (2007). "Heavy metal pollution and human biotoxic effects," *International Journal of Physical Sciences* 2(5), 112-118.
- Elaigwu, S. E., Rocher, V., Kyriakou, G., and Greenway, G. M. (2014). "Removal of Pb<sup>2+</sup> and Cd<sup>2+</sup> from aqueous solution using chars from pyrolysis and microwave-assisted hydrothermal carbonization of *Prosopis africana* shell," *Journal of Industrial and Engineering Chemistry* 20(5), 3467-3473. DOI: 10.1016/j.jiec.2013.12.036
- Förstner, U., and Wittmann, G. T. (1979). *Metal Pollution in the Aquatic Environment*, Springer-Verlag Berlin Heidelberg, Berlin, Germany. DOI: 10.1007/978-3-642-69385-4
- Foo, K. Y., and Hameed, B. H. (2010). "Insights into the modeling of adsorption isotherm systems," *Chemical Engineering Journal* 156(1), 2-10. DOI: 10.1016/j.cej.2009.09.013
- Guo, Y., Tang, W., Dai, J. Y., Hu, L. C., Zhu, Q. T., and Wang, L. (2014). "Influence of elution of biochar on its adsorption of Cu," *Journal of Agro-Environment Science* 33, 1405-1413 (in Chinese).
- Hu, X. J., Wang, J. S., Liu, Y. G., Li, X., Zeng, G. M., Bao, Z. L., Zeng, X. X., Chen, A. W., and Long, F. (2011). "Adsorption of chromium (VI) by ethylenediamine-modified cross-linked magnetic chitosan resin: Isotherms, kinetics and thermodynamics," *Journal of Hazardous Materials* 185(1), 306-314. DOI: 10.1016/j.jhazmat.2010.09.034
- Inyang, M., Gao, B., Yao, Y., Xue, Y., Zimmerman, A. R., Pullammanappallil, P., and Cao, X. D. (2012). "Removal of heavy metals from aqueous solution by biochars derived from anaerobically digested biomass," *Bioresource Technology* 110, 50-56. DOI: 10.1016/j.biortech.2012.01.072
- Inyang, M. I., Gao, B., Yao, Y., Xue, Y. W., Zimmerman, A., Mosa, A., Pullammanappallil, P., Ok, Y. S., and Cao, X. D. (2015). "A review of biochar as a low-cost adsorbent for aqueous heavy metal removal," *Critical Reviews in Environmental Science and Technology* 46(4), 406-433. DOI: 10.1080/10643389.2015.1096880

- Joseph, S., Graber, E. R., Chia, C., Munroe, P., Donne, S., Thomas, T., Nielsen, S., Marjo, C., Rutledge, H., Pan, G. X., *et al.* (2013). "Shifting paradigms: Development of high-efficiency biochar fertilizers based on nano-structures and soluble components," *Carbon Management* 4(3), 323-343. DOI: 10.4155/CMT.13.23
- Kim, W. K., Shim, T., Kim, Y. S., Hyun, S., Ryu, C., Park, Y. K., and Jung, J. (2013). "Characterization of cadmium removal from aqueous solution by biochar produced from a giant Miscanthus at different pyrolytic temperatures," *Bioresource Technology* 138: 266-270. DOI: 10.1016/j.biortech.2013.03.186
- Kloss, S., Zehetner, F., Dellantonio, A., Hamid, R., Ottner, F., Liedtke, V., Schwanninger, M., Gerzabek, M. H., and Soja, G. (2012). "Characterization of slow pyrolysis biochars: Effects of feedstocks and pyrolysis temperature on biochar properties," *Journal of Environmental Quality* 41(4), 990-1000. DOI: 10.2134/jeq2011.0070
- Lehmann, J. (2007), "A handful of carbon," *Nature* 447(7141), 143-144. DOI: 10.1038/447143a
- Lehmann, J., and Joseph, S. (2009). *Biochar for Environmental Management: Science and Technology*, Routledge, Abingdon-on-Thames, UK.
- Lu, H. L., Zhang, W. H., Yang, Y. X., Huang, X. F., Wang, S. Z., and Qiu, R. L. (2012). "Relative distribution of Pb<sup>2+</sup> sorption mechanisms by sludge-derived biochar," *Water Research* 46(3), 854-862. DOI: 10.1016/j.watres.2011.11.058
- Lu, R. (2000). *Analysis Methods of Soil Agricultural Chemistry*, China Agricultural Science and Technology Publishing House, Beijing, China (In Chinese).
- Mohammed, F. M., Roberts, E. P. L., Hill, A., Campen, A. K., and Brown, N. W. (2011). "Continuous water treatment by adsorption and electrochemical regeneration," *Water Research* 45(10), 3065-3074. DOI: 10.1016/j.watres.2011.03.023
- Mohan, D., Sarswat, A., Ok, Y. S., and Pittman, C. U. (2014). "Organic and inorganic contaminants removal from water with biochar, a renewable, low cost and sustainable adsorbent - A critical review," *Bioresource Technology* 160, 191-202. DOI: 10.1016/j.biortech.2014.01.120
- Nartey, O. D., and Zhao, B. (2014). "Biochar preparation, characterization, and adsorptive capacity and its effect on bioavailability of contaminants: An overview," *Advances in Materials Science and Engineering* (2014). DOI: 10.1155/2014/715398
- Qian, T., Wang, Y., Fan, T., Fang, G., and Zhou, D. (2016). "A new insight into the immobilization mechanism of Zn on biochar: the role of anions dissolved from ash," *Scientific Report*. 6, 33630. DOI: 10.1038/srep33630
- Ryan, J. A., Zhang, P., Hesterberg, D., Chou, J., and Sayers, D. E. (2001). "Formation of chloropyromorphite in a lead-contaminated soil amended with hydroxyapatite," *Environmental Science & Technology* 35(18), 3798-3803. DOI: 10.1021/es010634I
- Tan, X. F., Liu, Y. G., Zeng, G. M., Wang, X., Hu, X. J., Gu, Y. L., and Yang, Z. Z. (2015). "Application of biochar for the removal of pollutants from aqueous solutions," *Chemosphere* 125, 70-85. DOI: 10.1016/j.chemosphere.2014.12.058
- Uchimiya, M., Chang, S., and Klasson, K. T. (2011). "Screening biochars for heavy metal retention in soil: Role of oxygen functional groups," *Journal of Hazardous Materials* 190(1-3), 432-441. DOI: 10.1016/j.jhazmat.2011.03.063
- Wang, X. S., Lu, Z. P., Miao, H. H., He, W., and Shen, H. H. (2011). "Kinetics of Pb (II) adsorption on black carbon derived from wheat residue," *Chemical Engineering Journal* 166(3), 986-993. DOI: 10.1016/j.cej.2010.11.089
- Wang, Z. Y., Liu, G. C., Zheng, H., Li, F. M., Ngo, H. H., Guo, W. S., Liu, C., Chen, L.,

- and Xing, B. S. (2015). "Investigating the mechanisms of biochar's removal of lead from solution," *Bioresource Technology* 177, 308-317. DOI: 10.1016/j.biortech.2014.11.077
- Weber, W., and Morris, J. (1962). "Removal of biologically resistant pollutants from waste waters by adsorption," *Advances in Water Pollution Research* 2, 231-266.
- Wu, H., Yip, K., Kong, Z., Li, C. Z., Liu, D., Yu, Y., and Gao, X. (2011). "Removal and recycling of inherent inorganic nutrient species in mallee biomass and derived biochars by water leaching," *Industrial & Engineering Chemistry Research* 50, 12143-12151. DOI: 10.1021/ie200679n
- Xu, X. Y., Cao, X. D., Zhao, L., Wang, H. L., Yu, H. R., and Gao, B. (2013). "Removal of Cu, Zn, and Cd from aqueous solutions by the dairy manure-derived biochar," *Environmental Science and Pollution Research* 20(1), 358-368. DOI: 10.1007/s11356-012-0873-5
- Xu, Y. L., and Chen, B. L. (2014). "Organic carbon and inorganic silicon speciation in rice-bran-derived biochars affect its capacity to adsorb cadmium in solution," *Journal of Soil and Sediments* 15(1): 60-70. DOI: 10.1007/s11368-014-0969-2
- Yang, Y., Wei, Z. B., Zhang, X. L., Chen, X., Yue, D. M., Yin, Q., Xiao, L., and Yang, L. Y. (2014). "Biochar from *Alternanthera philoxeroides* could remove Pb(II) efficiently," *Bioresource Technology* 171, 227-232. DOI: 10.1016/j.biortech.2014.08.015
- Yuan, J. H., Xu, R. K., and Zhang, H. (2011). "The forms of alkalis in the biochar produced from crop residues at different temperatures," *Bioresource Technology* 102, 3488-3497. DOI: 10.1016/j.biortech.2010.11.018
- Zhang, A. F., Cui, L. Q., Pan, G. X., Li, L. Q., Hussain, Q., Zhang, X. H., Zheng, J. F., and Crowley, D. (2010). "Effect of biochar amendment on yield and methane and nitrous oxide emissions from a rice paddy from Tai Lake plain, China," *Agriculture Ecosystems & Environment* 139(4), 469-475. DOI: 10.1016/j.agee.2010.09.003
- Zhang, P., Sun, H. W., Yu, L., and Sun, T. H. (2013a). "Adsorption and catalytic hydrolysis of carbaryl and atrazine on pig manure-derived biochars: Impact of structural properties of biochars," *Journal of Hazardous Materials* 244, 217-24. DOI: 10.1016/j.jhazmat.2012.11.046
- Zhang, W. H., Mao, S. Y., Chen, H., Huang, L., and Qiu, R. L. (2013b). "Pb(II) and Cr(VI) sorption by biochars pyrolyzed from the municipal wastewater sludge under different heating conditions," *Bioresource Technology* 147, 545-52. DOI: 10.1016/j.biortech.2013.08.082
- Zheng, H., Wang, Z. Y., Deng, X., Herbert, S., and Xing, B. S. (2013). "Impacts of adding biochar on nitrogen retention and bioavailability in agricultural soil," *Geoderma* 206, 32-39. DOI: 10.1016/j.geoderma.2013.04.018
- Zhu, Q. H., Wu, J., Wang, L. L., Yang G., Zhang X. H. (2016). "Adsorption characteristics of Pb<sup>2+</sup> onto wine lees-derived biochar," *Bulletin of Environmental Contamination and Toxicology* 97(2), 294. DOI: 10.1007/s00128-016-1760-4

Article submitted: August 29, 2016; Peer review completed: October 29, 2016; Revised version received: January 4, 2017; Accepted: January 5, 2017; Published: January 18, 2017.

DOI: 10.15376/biores.12.1.1662-1679

## APPENDIX

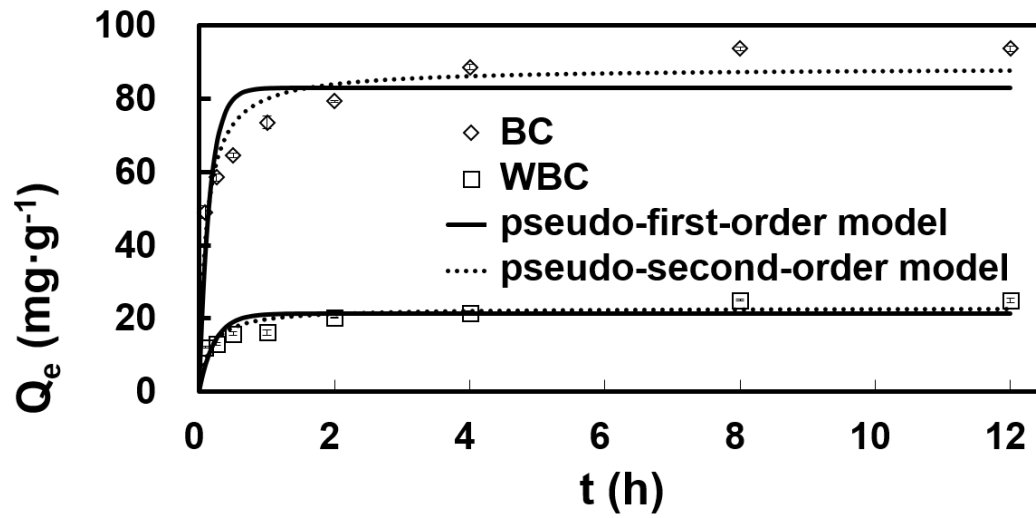


**Fig. S1.** Kinetic adsorption curves of Pb<sup>2+</sup> onto original biochar (BC) and water washed biochar (WBC).  $Q_e$  (mg g<sup>-1</sup>) is the amount of Pb<sup>2+</sup> sorbed at equilibrium

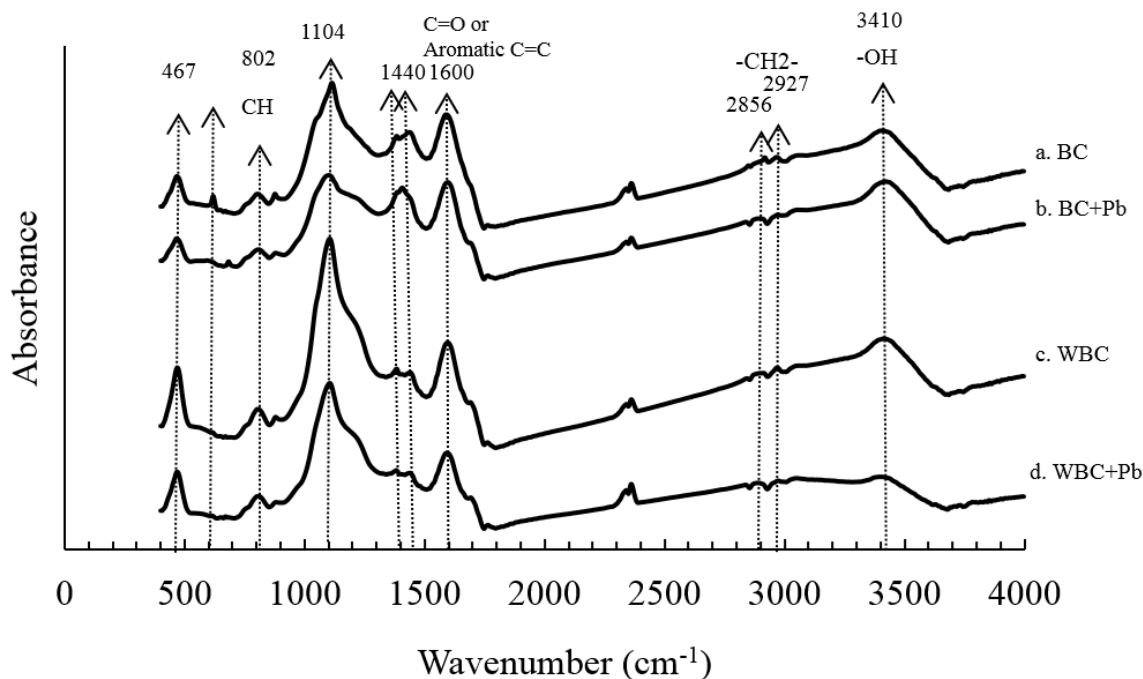


**Fig. S2.** FTIR spectra of BC and WBC before and after  $Pb^{2+}$  sorption

Figure S2 shows the FTIR spectra of BC and WBC before and after  $Pb^{2+}$  sorption. The broad peaks at  $3600\text{--}3300\text{ cm}^{-1}$  corresponded to O-H vibrations of hydroxyl groups. The peaks at  $2960\text{--}2850\text{ cm}^{-1}$  was assigned to aliphatic  $CH_2$  units, and the bands between  $873$  and  $721\text{ cm}^{-1}$  corresponded to aromatic CH (Wang *et al.* 2015). The peak located at  $1600\text{ cm}^{-1}$  was assigned to C=O of carboxyl and ketones or C=C aromatic components (Wang *et al.* 2015). The band at about  $1450\text{ cm}^{-1}$  (aromatic C=C ring stretching) and the peak at  $1400\text{ cm}^{-1}$  (corresponding to stretching vibration of the phenolic -OH or C-O stretching of carboxylate anion) (Silber *et al.* 2010; Wang *et al.* 2011) was lower in WBC than in BC. The broad band at  $1300\text{--}900\text{ cm}^{-1}$  (with peak at  $1104\text{ cm}^{-1}$ ) is assigned to Si-O-Si stretching vibration, and the two small bands at about  $802$  and  $467\text{ cm}^{-1}$  indicate Si-O-Si vibrations (Silber *et al.* 2010; Yang *et al.* 2008). The peaks of Si-O-Si increased in WBC compared to BC, which may be contributed the decrease of soluble minerals in biochar. The FTIR spectra demonstrated that biochar was constituted with organic and mineral phases. There were only small differences between water washed biochar and original biochar. These results demonstrated that washing with deionized water only removed the soluble ash and a small portion of dissolved organic carbon, but litter change the structure and surface functional groups of biochar, which was consistent with some other studies (Klasson *et al.* 2014; Wang *et al.* 2015; Zheng *et al.* 2013b).

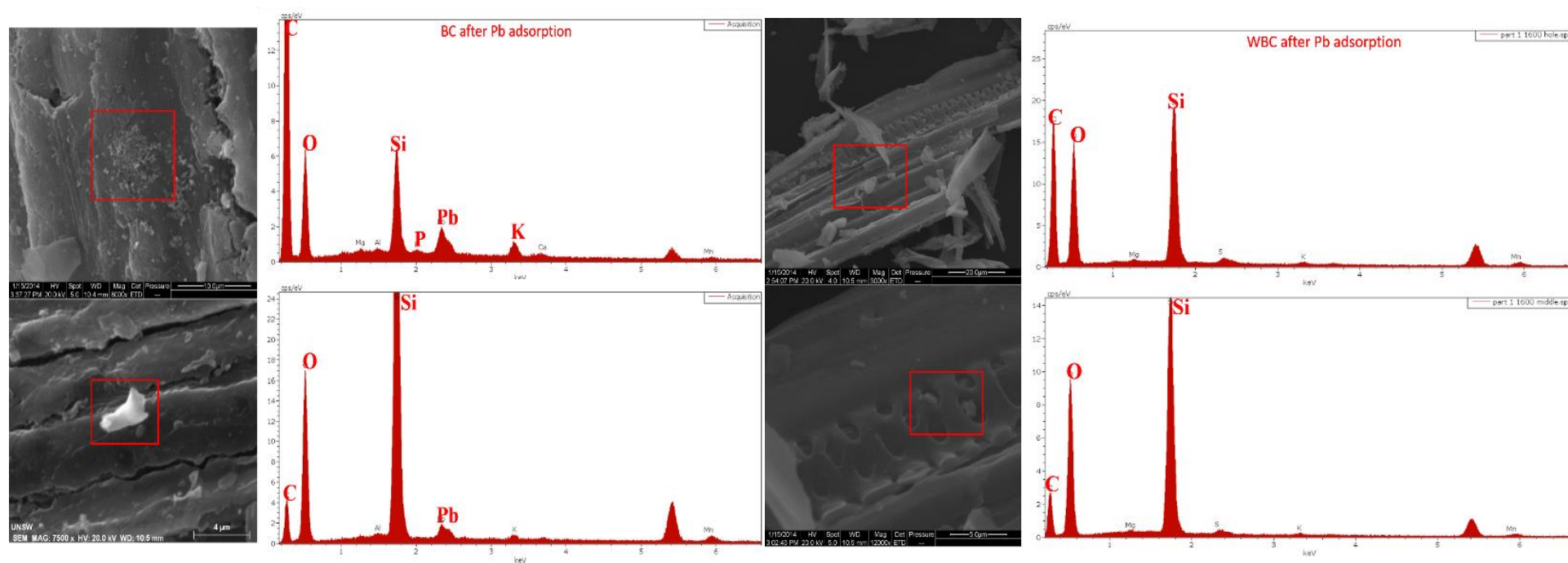


**Fig. S3.** SEM-EDS spectra for original biochar (BC, A-D) and water washed biochar (WBC, E-H). A and B are the SEM images of BC surface at a larger and smaller area, respectively after Pb adsorption; C and D are the corresponding EDS spectra collected from the boxed regions; E and F are the SEM images of WBC surface at a larger and smaller area, respectively after Pb adsorption; G and H are the corresponding EDS spectra collected from the boxed regions.

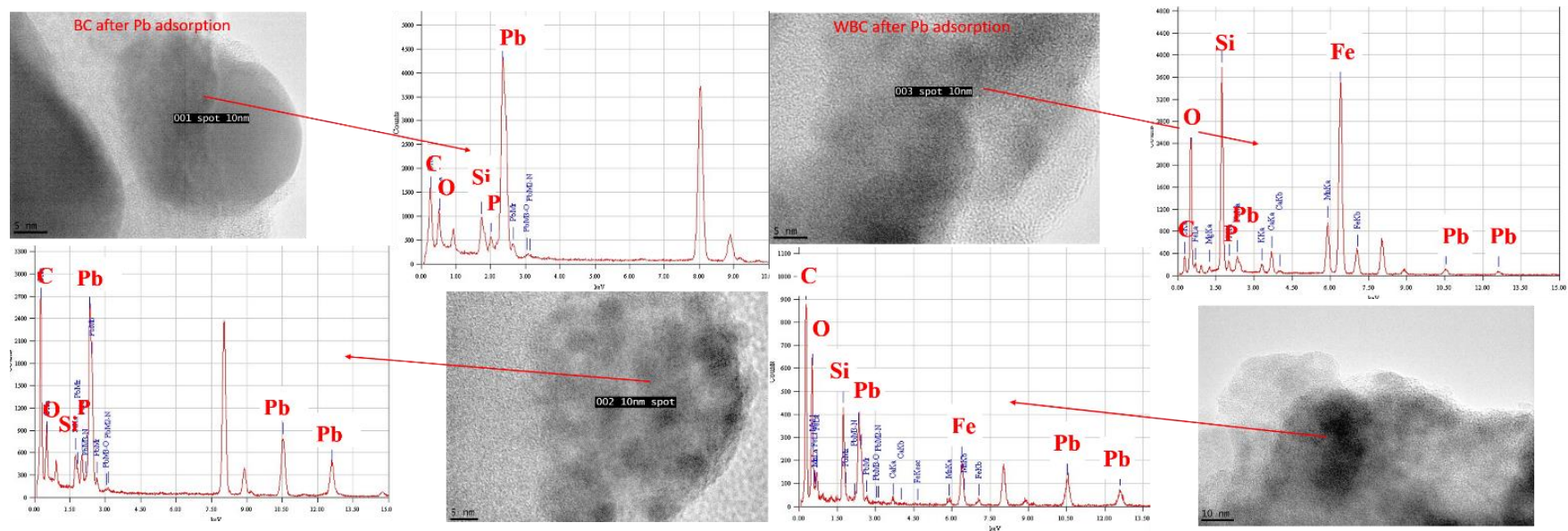


Fig. S4. TEM-EDS spectra of original biochar (BC, left) and water washed biochar (WBC, right)